

# Liver-Specific Overexpression of the Insulin-like Growth Factor-I Enhances Somatic Growth and Partially Prevents the Effects of Growth Hormone Deficiency

Lan Liao, Robert K. Dearth, Suoling Zhou, Ora L. Britton, Adrian V. Lee, and Jianming Xu

Department of Molecular and Cellular Biology (L.L., S.Z., A.V.L., J.X.) and Department of Medicine and Breast Cancer Center (R.K.D., O.L.B., A.V.L.), Baylor College of Medicine and Methodist Hospital, Houston, Texas 77030

The precise role of circulating IGF-I in somatic growth under normal and GH-deficient conditions remains unclear. To define the contribution of circulating IGF-I to the endocrine regulation of somatic growth and the GH/IGF-I axis, we constructed a transgene with the transthyretin (TTR) enhancer/promoter and the mouse IGF-I cDNA and generated TTR-IGF-I transgenic mice. The transgene was exclusively expressed in the liver, which resulted in a 50–60% increase in serum IGF-I, a decrease in serum GH, and an improved tolerance to glucose challenge. The body weight and lean mass of TTR-IGF-I mice were heavier compared with wild-type (WT) mice. The increase in lean mass was a result of increase in both number and thickness of skeletal muscle fibers. The femur, tibia, and body lengths of TTR-IGF-I mice also were longer. In WT mice, the GH antagonist pegvisomant (Peg) suppressed the transcription of endogenous IGF-I and acid-labile subunit (ALS) genes with no effect on IGF-binding protein 3

(IGFBP-3) mRNA. Consequently, Peg-induced GH deficiency in WT mice severely reduced ALS, IGF-I, and IGFBP-3 in the circulation and caused a severe growth deficit. In TTR-IGF-I mice, Peg reduced the mRNA of the endogenous IGF-I gene with no effect on the TTR-IGF-I transgene expression, leading to a blunted decrease in serum IGF-I levels. Interestingly, IGFBP-3 mRNA was elevated and circulating IGFBP-3 was less reduced in Peg-treated TTR-IGF-I mice. Peg-treated TTR-IGF-I mice also exhibited heavier body weight and longer body length than Peg-treated WT mice. Therefore, liver-expressed IGF-I can stimulate IGFBP-3 mRNA expression and stabilize IGFBP-3 under GH deficiency, leading to a better maintenance of IGF-I levels in the circulation. Higher circulating levels of IGF-I can stimulate somatic growth and lean mass and improve glucose tolerance. (*Endocrinology* 147: 3877–3888, 2006)

**M**ULTIPLE LINES OF evidence have confirmed the essential role of IGF-I in regulating postnatal somatic and bone growth and in mediating the somatotrophic function of GH (1, 2). For instance, GH induces IGF-I expression in multiple tissues and increases IGF-I levels in circulation, and inactivation of the IGF-I gene in mice severely impairs somatic growth after birth (1–4). IGF-I exerts its cellular function by binding to the extracellular domain of the  $\alpha$ -subunit of the IGF-I receptor (IGF-IR) complex and activating the intracellular tyrosine kinase domain of the  $\beta$ -subunit of IGF-IR, which triggers the transphosphorylation of IGF-IR $\beta$  subunits and activates its downstream signaling pathways (1, 2). Because both IGF-I and IGF-IR are widely expressed in different tissues, IGF-I may act on its target cells through endocrine, paracrine, and/or autocrine mechanisms. Therefore, it has been difficult to define the contribution of circulating IGF-I to somatic growth in response to GH stimulation. In the circulation, most IGF-I associates with IGF-binding protein 3 (IGFBP-3) and acid-labile subunit (ALS) to form a ternary complex, which remarkably extends the half-life of IGF-I and IGFBP-3 in the circulation and efficiently

maintains the reservoir of IGF-I and its endocrine function (1, 2). Consistent with this, overexpression of IGFBP-3 led to an increase in plasma IGF-I in transgenic mice (5). Conversely, a reduction of IGF-I in mice caused a reduction of circulating IGFBP-3 levels without affecting its mRNA expression in the liver (6). Null mutation of the ALS gene in mice also caused a significant decrease of IGF-I and IGFBP-3 in the circulation without affecting their mRNA transcription (7). These studies indicate that ALS is required for the stability of both IGF-I and IGFBP-3, whereas IGF-I and IGFBP-3 are required for each other's stability. These associated changes among the components of the ternary complex make it difficult to assess the specific role of systemic IGF-I in somatic growth.

The liver is the principle organ that produces circulating IGF-I, IGFBP-3, and ALS (1, 2). ALS is exclusively expressed in the liver, and its expression is dependent on GH stimulation. GH also directly stimulates IGF-I mRNA expression in the liver. The transcriptional regulation of IGFBP-3 in the liver is unclear, although some studies suggest that GH may indirectly regulate IGFBP-3 expression through enhancing IGF-I production (8, 9). Earlier studies showed that IGF-I could stimulate growth of pituitary-deficient rats, suggesting that the endocrine action of IGF-I was to promote somatic growth (10–12). However, this concept was challenged by a study demonstrating that deletion of the liver IGF-I gene in mice resulted in a 75% reduction in total plasma IGF-I levels, but mice exhibited normal growth (6). This study suggested that normal body growth might be mainly mediated by au-

First Published Online May 18, 2006

Abbreviations: ALS, Acid-labile subunit; GHR, GH receptor; IGFBP-3, IGF-binding protein 3; IGF-IR, IGF-I receptor; RPA, RNase protection assay; SRC-3, steroid receptor coactivator-3; SV40, simian virus 40; TBS, Tris-buffered saline; TTR, transthyretin; WT, wild type.

*Endocrinology* is published monthly by The Endocrine Society (<http://www.endo-society.org>), the foremost professional society serving the endocrine community.

tocrine/paracrine actions of IGF-I. However, two concerns of this animal model were the significantly elevated GH levels and the lack of reduction in free IGF-I levels in the circulation (6, 13). Interestingly, ALS null mice with a 65% reduction of circulating IGF-I levels but without change of GH levels exhibited a 13% growth deficit (7), suggesting that the endocrine action of IGF-I does play a role in the regulation of somatic growth. The difference between growth in liver-specific IGF-I knockout mice and ALS knockout mice may be the result of a higher turnover of IGF-I in ALS knockout mice and thus reduced bioavailability. Importantly, disruption of both the liver IGF-I and ALS genes resulted in a 30% decrease in body weight, further substantiating the role for circulating IGF-I in body growth (14). Although these loss-of-function animal models provide great insight into the understanding of the endocrine function of the liver-generated or systemic IGF-I, a gain-of-function animal model with liver-specific and GH-independent production of IGF-I may provide additional insight into understanding the role of circulating IGF-I in the regulation of the GH/IGF-I axis, somatic growth, and carcinogenesis.

In the present study, we have generated transthyretin (TTR)-IGF-I transgenic mice with TTR gene enhancer/promoter-directed liver-specific expression of a mouse IGF-I transgene. We show that these mice have a significant increase in their plasma IGF-I levels, which is accompanied by increases in body weight, body length, bone length, and lean mass, improved glucose tolerance, and partially suppressed serum GH levels. In wild-type (WT) mice, blockade of the GH receptor (GHR) by pegvisomant treatment diminished ALS mRNA in the liver and ALS protein in the blood, reduced IGF-I mRNA in the liver and IGF-I protein in the blood, and reduced IGFBP-3 protein in the blood without changing IGFBP-3 mRNA in the liver. These alterations were accompanied by severe growth deficit. Interestingly, in the IGF-I transgenic mice treated with pegvisomant, the IGFBP-3 mRNA levels in the liver and the plasma levels of IGF-I and IGFBP-3 were much higher compared with pegvisomant-treated WT mice. Pegvisomant-treated TTR-IGF-I mice also exhibited heavier body weight and longer body length than pegvisomant-treated WT mice. These results indicate that the liver-produced IGF-I can promote somatic growth under both normal physiological and GHR-dysfunctional conditions. Importantly, the liver-produced IGF-I also can stabilize IGFBP-3 and stimulate IGFBP-3 transcription under GH-deficient conditions, which may facilitate the maintenance of IGF-I concentration and endocrine function and thereby increase the resistance to GH deficiency.

## Materials and Methods

### Construction of the IGF-I transgene

Total RNA sample was prepared from C57BL/6J mouse liver and reverse transcribed into cDNA as templates for PCR. The mouse IGF-I cDNA was amplified by PCR using a pair of mouse IGF-I-specific primers with *Acc65I* and *EcoR1* cloning sites, 5'-TATAGGTACCCACTCTGACCTGCTGTG (IGF-I forward) and 5'-TATAGAATTTCGATGTTTTCAGGTTGCTC (IGF-I reverse). The PCR-amplified 600-bp IGF-I cDNA was subcloned into the pBluescript II SK plasmid, and its authenticity was verified by DNA sequence analysis. Subsequently, the *Acc65I/EcoR1* fragment was transferred into the PAP-TTR-SV plasmid that contained a TTR promoter and a simian virus 40 (SV40) polyade-

nylation signaling sequence. The *Asc1/Pac1* TTR-IGF-I-SV fragment was then transferred into the PAP-2xHS4-2xHS4 plasmid (15) with two repeats of the HS4 chromatin insulation sequence on each side of the *Asc1* and *Pac1* sites (Fig. 1A). The vector backbone was removed by *NotI* digestion. The 6-kb transgene DNA was gel purified and microinjected into the pronuclei of fertilized eggs of C57BL/6J mice. Microinjected eggs were transferred into the uteri of pseudopregnant female mice and allowed to develop to term.

### Genotyping and estimation of the transgene copy numbers

Pups derived from embryo transfer were screened for positive transgene founders at the age of 3 wk by PCR-based genotyping using genomic DNA samples prepared from tail tip biopsy. The forward primer (5'-ATGTCGTCCTCACACCTCTTCT) and the reverse primer (5'-TTCGATGTTTTGCAGGTTGCTC) for PCR were located in exons 2 and 4 of the IGF-I gene, respectively. PCR was performed with the following program: 94 C for 3 min, 56 C for 1 min, and 72 C for 1 min for one cycle; 94 C for 50 sec, 56 C for 50 sec, and 72 C for 1 min for 38 cycles; and 94 C for 50 sec; 56 C for 50 sec, and 72 C for 3 min for one cycle. PCR product was analyzed by 1.5% agarose gel electrophoresis.

A comparative PCR method was used to estimate the copy number of the IGF-I transgene. Genomic DNA isolated from WT and transgenic mice were used as PCR templates. Both endogenous and transgene were amplified by the same pair of primers, 5-CCACAGGCTATGGCTC-CAGC and 5'-AGTCTTGGGCATGTCAGTGTG, which produced a 190-bp amplicon. The results were normalized by coamplification of the endogenous steroid receptor coactivator-3 (SRC-3) gene by another pair of primers as described (16). The copy number of the IGF-I transgene was estimated by comparing the relative ratio of IGF-I to SRC-3 gene products in transgenic mice containing two endogenous IGF-I alleles and transgene alleles with the relative ratio of IGF-I to SRC-3 gene products in WT mice with two endogenous IGF-I alleles.

### RNase protection assay (RPA)

Total RNA was extracted from WT and IGF-I transgenic mouse livers by using the Trizol reagent (Invitrogen, Hercules, CA). [<sup>32</sup>P]UTP-labeled riboprobes were transcribed by the MAXIScript T7 kit (Ambion, Austin,

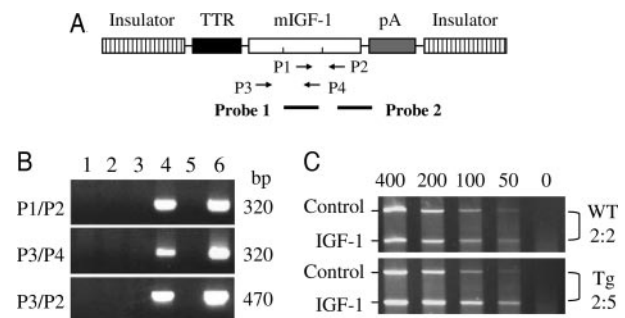


**FIG. 1.** Generation of IGF-I transgenic mice. **A**, Transgene construct. The transgene contains the enhancer/promoter region of TTR, the mIGF-I cDNA and the SV40t polyadenylation signal sequence (pA). The transgene is flanked by chromosomal insulator sequences. Each insulator contains two repeats of the HS4 sequence. The locations for two exon/exon junctions in the mIGF-I cDNA (short sticks), four PCR primers (P1–P4) and two RPA probes (probes 1 and 2) are indicated. **B**, Identification of IGF-I transgenic mice. Tail DNA was prepared from WT control (lane 1) and mice derived from microinjected embryos (lanes 2–5). PCR analyses were performed with indicated primer pairs and tail DNA (lanes 1–5) or the positive control plasmid with the transgene (lane 6). **C**, Estimation of TTR-IGF-I transgene copies. Semiquantitative PCR was performed with the indicated amount (ng) of genomic DNA prepared from WT and heterozygous TTR-IGF-I (Tg) mice. The control band was detected by a pair of primers specific to the mouse SRC-3 gene. The IGF-I band was detected by P1/P4 primers shown in the **A**. P1/P4 primers could detect both endogenous and transgenic IGF-I alleles. The estimated ratios of the IGF-I band intensity to the control band intensity are indicated.

TX). RPA was performed with 15  $\mu$ g total RNA by using the RPA III kit (Ambion). The RNase-protected bands were detected by running 6% denaturing polyacrylamide gel at 330 V and by exposing dried gel to x-ray film at  $-80^{\circ}\text{C}$ .

Two riboprobes were generated to detect the endogenous IGF-I mRNA and the IGF-I mRNA transcribed from the transgene. The DNA template for the first probe was complementary to the exon 3 of the IGF-I gene, and it was amplified from reverse transcribed mouse liver cDNA by PCR using the following primers: 5'-CCACAGGCTATGGCTC-CAGC and 5'-GTAATACGACTCACTATAGGGCGAATTGGGTAGTC-TTGGGCATGTCAGTGTG (*italic, T7; underlined*, a sequence taken from the pBluescript II SK plasmid). The transcribed probe was 180 bp in length, and its protective length was 170 bp. This probe was able to equally hybridize with both endogenous and transgenic IGF-I mRNA. The second riboprobe was designed to distinguish the transgenic IGF-I mRNA from the endogenous IGF-I mRNA. The 5' portion of its sequence was complementary to IGF-I mRNA, but the 3' portion of its sequence was specific to the SV40 polyadenylation signaling sequence of the transgene. The template of this probe was amplified by PCR using primer T1 (ACAAGTAGAGGAAGTGCAG) and T2 (GTAATACGA CT-CACTATAGGGCGAATTGGGTGATCCCCGGGCTGCAGGAA). The transcribed probe was 150 bp in length. The protective lengths for endogenous and transgenic IGF-I mRNAs were 120 and 140 bp, respectively.

The DNA template of the IGFBP-3 riboprobe was amplified from reverse transcribed mouse liver cDNA by PCR using primer P149 (ACATCAGTGAGTCCAAGGAG) and P151 (GTAATACGACTCACTA-TAGGGCGAATTGGGTAGCGCTGGCTGTCCCTGGCG). The length of the transcribed probe was 160 bp, and its protective length was 150 bp. The DNA template of the ALS riboprobe was amplified from reverse transcribed mouse liver cDNA by PCR using primer ALS-P1 (GTGT-TCCAAGGGCTGGGCAG) and ALS-P3 (GTAATACGACTCACTATAG-GGCGAATTGGGTGGAGATGCTGTGTCCCGGA). Its transcribed length was 140 bp, and its protective length was 130 bp.

## RIA

IGF-I assay was carried out as previously described (16). Briefly, total IGF-I was extracted from serum and measured by using the rat IGF-I RIA kit (Diagnostic Systems Laboratories, Webster, TX). Samples, standards, and controls were incubated with  $^{125}\text{I}$ -labeled IGF-I and antibodies against IGF-I according to the manufacturer's protocol. The IGF-I and antibody complexes were precipitated, and its  $^{125}\text{I}$  radioactivity was counted on a  $\gamma$ -counter. The IGF-I concentration in serum samples was determined against the standard curve.

For GH measurement, mice were bled at 0800 h on d 1, 1500 h on d 14, and 2200 h on d 21. This schedule was designed based on the limiting mice blood volume and the fluctuation feature of GH secretion. The serum GH concentration was measured by using the Rat GH Assay Kit (Amersham Pharmacia, Piscataway, NJ), but the GH antibody in the kit was replaced by a rabbit anti-rGH antiserum (1:100,000 dilution) provided by Dr. A. F. Parlow (National Hormone and Peptide Program, Torrance, CA). The average value of three samples from a mouse was used to represent the GH level for this mouse. Insulin was measured by using the Sensitive Rat Insulin RIA Kit (Linco Research, St. Charles, MO).

## Measurement of body weight, body length, bone length, lean mass, and fat mass

The mouse body weight was measured once a week by using an electronic scale. The mouse body length from the tip of nose to the bottom of the tail was measured under anesthesia at the end points of experiments with a ruler. Femur and tibia bone length was measured using a Faxitron Specimen Radiography System from DALSA Life Sciences (Tucson, AZ). Beginning at 5 wk of age, mice were x-rayed under anesthesia every 2 wk until 11 wk old, and bone length measurements (in millimeters) were acquired using the Faxitron computer ruler program. Femur length was determined by starting at the femoral head to the formation of the genu joint at the medial and lateral condyles. The tibia was measured from the cranial intercondylar area to the medial malleolus. At 13 wk of age, mice were anesthetized and body mass composition was analyzed by dual-energy x-ray absorptiometry den-

sitometry using a PIXImus II Densitometer (Lunar Corp., Madison, WI) as previously described (17).

## Muscle histology

Adult male mice (5–6 months old) were killed, and the hind-limb muscle soleus was isolated together with its connecting bones. After being fixed in 4% paraformaldehyde in PBS overnight at  $4^{\circ}\text{C}$ , the soleus muscle was washed in PBS, cut into two segments in the middle, and embedded in paraffin. Cross-sections were prepared from the thickest portion of the muscle and stained with hematoxylin and eosin for histological examination. The muscle sections were analyzed as previously described (18). The electronic images of muscle cross-sections were recorded under a 5-fold microscope objective. The area (pixels) of each muscle cross-section was measured by using NIH Image 1.62 Allas software, and the number of muscle fibers was counted by using the UTHSCSA Image Tool software. The average thickness of muscle fibers in the soleus was calculated by dividing the cross-sectional area with the total number of muscle fibers.

## Glucose measurement and glucose and insulin tolerance tests

Adult WT and TTR-IGF-I male mice (5–6 months) were fasted for 6 h. Blood glucose levels were measured by collecting one drop of blood from the tail and using the One Touch Ultra Glucose Meter (LifeScan, Inc., Milpitas, CA). For the glucose tolerance test, ip injection of glucose (200 mg/ml in saline, using 2 g/kg body weight) was performed, and the mouse blood glucose levels were measured at 15, 30, 60, and 120 min after the injection. For the insulin tolerance test, ip injection of insulin (0.05 U/ml in saline, using 0.5 U/kg body weight) was performed after the basal glucose level was measured. After insulin injection, mouse glucose levels were measured at 15, 30, 60, and 120 min. After the time course was finished, mice were injected with 0.2 ml glucose solution (200 mg/ml in saline, ip injection) for recovery.

## Pegvisomant treatment

Pegvisomant was a generous gift from Pfizer (Cambridge, MA). The buffered pegvisomant was resuspended in water at 20 mg/ml and stored at  $4^{\circ}\text{C}$  until use within a week. Three-week-old WT and IGF-I transgenic mice were injected with pegvisomant (ip, 250 mg/kg) or an equal volume of PBS (vehicle) at 0900 h on every other day. Mice were treated for 5 consecutive weeks. Mice were weighed every time before injection. Blood samples were collected for IGF-I and GH measurement at the second, fourth, and fifth week of pegvisomant treatment. At the end of treatment, mice were killed and the weight of their brain, pituitary, heart, liver, and kidney was measured.

## Ligand blotting analysis

The level of serum IGFBP-3 was assayed by ligand blotting analysis as previously described (7, 14, 19). Briefly, 0.5  $\mu$ l serum was mixed with nonreducing SDS-PAGE sample buffer, heat-denatured, and separated by running a 10% SDS-PAGE mini-gel at 100 V. Proteins were blotted to nitrocellulose membrane, and the membrane was washed with PBS and then incubated with PBS containing 3% Nonidet P40 for 30 min at  $4^{\circ}\text{C}$ . The membrane was blocked with 1% BSA (fraction V, RIA grade, catalog no. A-7888; Sigma Chemical Co., St. Louis, MO) in PBS at  $4^{\circ}\text{C}$  for 2 h and then washed for 10 min at  $4^{\circ}\text{C}$  in PBS containing 0.1% Tween 20. The membrane was subsequently incubated at  $4^{\circ}\text{C}$  overnight in 5 ml PBS containing 1% RIA-grade BSA, 0.1% Tween 20, and  $5 \times 10^5$  cpm of the  $^{125}\text{I}$ -labeled recombinant human IGF-I (receptor grade; Diagnostic Systems Laboratories) in a sealed plastic bag. The membrane was washed two times with PBS containing 0.1% Tween 20 and three times with PBS, air dried, wrapped with plastic membrane, and exposed to x-ray film for 2–3 d at  $-80^{\circ}\text{C}$ .

## Western blot analysis

The ALS antibody (AF1436; R&D Systems, Minneapolis, MN) was used in Western blot analysis as described previously (20). Briefly, mouse serum was mixed with SDS-PAGE reducing sample buffer,

boiled, and separated by 10% SDS-PAGE. Proteins were transferred to nitrocellulose membrane. The membrane was blocked in Tris-buffered saline (TBS) containing 5% fat-free dry milk powder for 30 min at room temperature or overnight at 4 C. Then, the membrane was incubated in TBS containing 1% BSA and the ALS antibody for 1 h at room temperature. After washing with TBS, the membrane was incubated in TBS containing 1% BSA and a secondary antibody (1:5000 dilution) conjugated with horseradish peroxidase for 1 h at room temperature. The membrane was washed in TBS, developed for 1 min in 2 ml ECL solution (Amersham), and exposed to x-ray film.

## Results

### Generation of the liver-specific IGF-I transgenic mice

The aim of this study was to define the role of elevated circulating IGF-I on the GH/IGF-I regulatory axis and somatic growth under both natural and impaired GH signaling conditions. The major source of systemic IGF-I is synthesized in, and secreted from, the liver and regulated by GH (1, 2). To express IGF-I in a liver-specific and GH-independent manner, we constructed a transgene consisting of the enhancer/promoter of the TTR gene, the mouse IGF-I cDNA, and the SV40t polyadenylation-signaling sequence (Fig. 1A). The TTR enhancer/promoter has been shown to target transgene expression specifically to the liver (15, 21, 22). To minimize the positional effect of chromosomal integration sites on transgene expression, the IGF-I transgene was flanked with a tandem repeat of the HS4 chromosomal insulator sequence from the 5' region of the chicken  $\beta$ -globin gene (23). Transgene DNA was isolated and microinjected into fertilized eggs prepared from C57BL/6 mice to produce transgenic founder mice.

TTR-IGF-I transgenic founder mice were identified by PCR analysis using DNA samples isolated from the tail tips. PCR analyses using nested primer pairs spanning two or more exon-exon junctions revealed that this transgenic line harbored the full-length IGF-I transgene (Fig. 1B, lane 4). These primers specifically detected the TTR-IGF-I transgene because PCR using these primer pairs and *Taq* DNA polymerase was unable to amplify the products containing large introns from the endogenous IGF-I alleles. The transgenic colony was established by crossing the male founder with C57BL/6 female mice. The established line was maintained as heterozygous TTR-IGF-I transgenic mice. Both heterozygous and homozygous TTR-IGF-I transgenic mice exhibited normal development and normal reproductive function.

Next, we estimated the transgene copy number by semi-quantitative PCR analysis. When a serial dilution of genomic DNA from WT mice was used as PCR template, PCR products of the reference gene and the IGF-I gene were equally amplified because there were two alleles for both genes in WT mice (Fig. 1C, *top*). The reference band was detected by a pair of primers located in an exon of the SRC-3 gene (16). The IGF-I band was detected by P1 and P4 primers located in the exon 3 of the IGF-I gene (Fig. 1A), so they could detect both the endogenous IGF-I gene and the transgenic TTR-IGF-I gene. When a serial dilution of genomic DNA from the TTR-IGF-I mice was used for PCR analysis, the amount of reference product was the same as that amplified from WT mice. However, the intensity of the IGF-I band amplified from TTR-IGF-I mice with both IGF-I WT and TTR-IGF-I transgenic alleles was much stronger than that amplified

from WT mice. The ratio of the IGF-I band intensity to the reference band intensity was about 5:2. Therefore, we estimated that there are approximately three copies of the TTR-IGF-I transgene in the TTR-IGF-I heterozygous mice.

### Liver-specific expression of the TTR-IGF-I transgene causes an increase in IGF-I and a decrease in GH in the circulation

The expression profile of the TTR-IGF-I transgene was examined by RPA analysis of RNA samples isolated from different organs including brain, heart, liver, kidney, spleen, and skeletal muscle. A  $^{32}$ P-labeled riboprobe, probe 1 shown in Fig. 1A, complementary to a common region of the endogenous and transgenic IGF-I mRNA detected a strong band from the liver RNA and a weak band from RNA samples isolated from other organs of WT mice. The same probe detected a 4-fold stronger band from the liver RNA of the TTR-IGF-I transgenic mice, and the relative intensity of the protected IGF-I bands from RNA samples of other organs stayed the same as compared with WT mice (Fig. 2A). These results suggested that the TTR-IGF-I transgene is specifically expressed in the liver at a higher level than the endogenous IGF-I gene. To further analyze the expression profile and levels of the TTR-IGF-I transgene, we designed another riboprobe (probe 2 in Fig. 1A) consisting of the 3' IGF-I coding region that was common to both endogenous and transgenic IGF-I mRNAs and the 5' SV40t polyadenylation-signaling sequence that was unique for the transgenic mRNA. This riboprobe should distinguish the TTR-IGF-I transgene expression (full-length protection) from the endogenous IGF-I expression (partial region protection). Indeed, this second riboprobe not only detected the equal expression levels of the endogenous IGF-I mRNA in livers of both WT and TTR-IGF-I transgenic mice but also detected the exclusive expression of the TTR-IGF-I transgene in the liver of the TTR-IGF-I transgenic mice. The expression level of the TTR-IGF-I transgene was about 3-fold higher than the endogenous IGF-I gene (Fig. 2B). These results indicate that the TTR-IGF-I transgenic mice with liver-specific overexpression of IGF-I were successfully developed.

To examine whether the liver-specific expression of the TTR-IGF-I transgene would change the circulating levels of IGF-I, serum IGF-I concentrations were measured by RIA. The average concentrations of total serum IGF-I were  $468 \pm 55$  and  $432 \pm 68$  ng/ml in 8- to 12-wk-old male and female WT mice, respectively. In the same age male and female TTR-IGF-I transgenic mice, the average concentrations of serum IGF-I were  $696 \pm 108$  and  $693 \pm 102$  ng/ml, which were significantly increased by 50 and 60% compared with male and female WT mice, respectively (Fig. 2C). These results indicate that the liver-specific expression of the TTR-IGF-I transgene significantly increases IGF-I levels in the circulation.

To examine whether the increased IGF-I would suppress GH secretion, we collected blood samples from adult male WT and TTR-IGF-I mice for GH analysis. Given the pulsatile fashion of GH secretion and the limited volume of the mouse blood pool, we bled each mouse once every other week at three different time points (see *Materials and Methods*) and

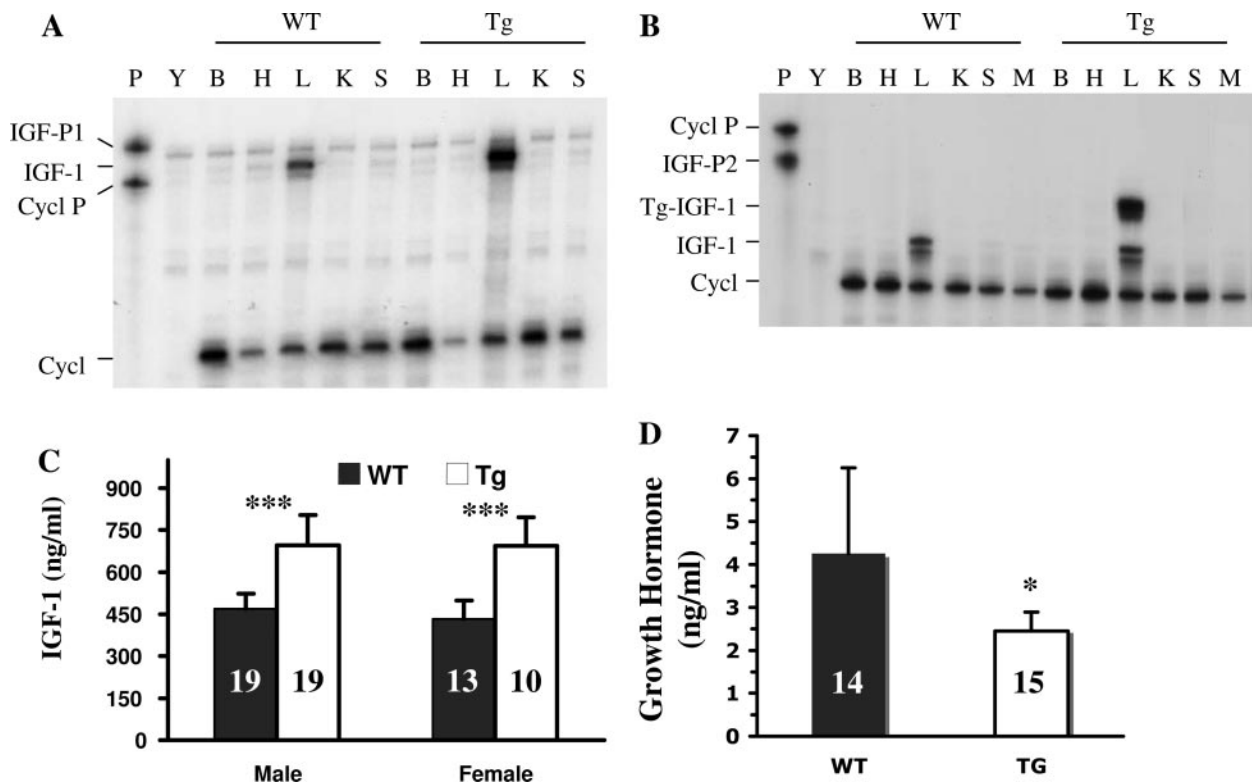


FIG. 2. Liver-specific overexpression of the TTR-IGF-I transgene leads to elevation of serum IGF-I levels and reduction of GH. A, RPA analysis using the probe 1 shown in Fig. 1A. RNA was extracted from the pituitary (P), brain (B), heart (H), liver (L), kidney (K), and spleen (S) of WT and TTR-IGF-I transgenic (Tg) mice. Fifteen micrograms of tissue RNA or yeast (Y) RNA (negative control) were used for each assay. The full-length riboprobes (P) including the probe 1 of IGF-I (IGF-P1) and the cyclophilin A probe (Cycl P) and the protected IGF-I mRNA (IGF-I) and cyclophilin mRNA (Cycl) bands are indicated. Note the specific increase of the protected IGF-I mRNA band in TTR-IGF-I (Tg) mice, which represents the sum of endogenous and transgenic IGF-I mRNAs. B, RPA analysis using the IGF-I probe 2 (IGF-P2) shown in Fig. 1A. RNA samples were extracted from the same types of tissues indicated in A and from skeletal muscle (M). Note the comparable intensity of the protected endogenous IGF-I mRNA in WT and TTR-IGF-I (Tg) mice and the liver-specific overexpression of the transgenic IGF-I mRNA (Tg-IGF-I) in the TTR-IGF-I (Tg) mice. C, Elevation of serum IGF-I in TTR-IGF-I mice. Serum samples were prepared from 8- to 12-wk-old male WT ( $n = 23$ ) and TTR-IGF-I (Tg) ( $n = 20$ ) mice as well as female WT ( $n = 13$ ) and TTR-IGF-I (Tg) ( $n = 5$ ) mice. Data are presented as mean  $\pm$  SD. \*\*\*,  $P < 0.001$  by  $t$  test between male or female WT and Tg mice. D, Reduction of GH in TTR-IGF-I mice. Serum samples for each male mouse (5–6 months old) were prepared from bleeding at three time points (see *Materials and Methods*) and individually assayed by RIA. A total of 14 WT and 15 TTR-IGF-I mice were analyzed. Data are presented as average  $\pm$  SD. \*,  $P < 0.05$  by unpaired  $t$  test.

measured GH levels in these individual samples. We assayed 14 WT and 15 TTR-IGF-I male adult mice and found that the average GH levels in TTR-IGF-I mice were significantly lower than in WT mice (Fig. 2D), suggesting that the elevated IGF-I from the TTR-IGF-I transgene is biologically active and plays a role in negative-feedback regulation of GH levels in the circulation.

#### Liver-specific expression of the TTR-IGF-I transgene increases body weight, lean mass, and bone length

To address the question as to whether the elevation of plasma IGF-I levels by the liver-specific transgene would stimulate somatic growth, the body weight of WT and TTR-IGF-I transgenic mice was measured. The measurement started at the age of 2 wk and ended at the age of 12 wk. Most measured and compared WT and TTR-IGF-I transgenic mice were littermates derived from breeding pairs of WT and TTR-IGF-I heterozygous mice. The male TTR-IGF-I mice started to grow faster than male WT mice at the age of 5 wk, and their average body weight became significantly heavier than male WT mice at 9 wk and older ages (Fig. 3A). The

female TTR-IGF-I mice also grew faster than female WT mice. The average body weight of female TTR-IGF-I mice was significantly heavier than the average body weight of female WT mice at the ages of 8, 10, 11, and 12 wk (Fig. 3A). To find out what caused the increase in the body weight of TTR-IGF-I mice, lean mass and fat mass were measured. The lean masses of 13-wk-old WT and TTR-IGF-I female mice were  $16.17 \pm 0.56$  g/mouse ( $n = 10$ ) and  $16.93 \pm 0.53$  g/mouse ( $n = 10$ ), respectively. The lean mass of TTR-IGF-I mice was statistically heavier than the lean mass of WT mice ( $P = 0.01$ , unpaired  $t$  test). In contrast, the fat masses of WT and TTR-IGF-I mice were not significantly different, which were  $1.86 \pm 0.26$  g/WT mouse ( $n = 10$ ) and  $1.90 \pm 0.18$  g/TTR-IGF-I mouse ( $n = 10$ ). Taken together, these results indicate that the elevated systemic IGF-I originated from the liver-specific expression of the TTR-IGF-I transgene can significantly stimulate somatic growth and lean mass increase.

Next, we examined the histology of soleus, a hind-limb skeletal muscle, in adult male mice (5–6 months old) to address the feature of lean mass increase in TTR-IGF-I mice. Examination of soleus cross-sections revealed that the entire

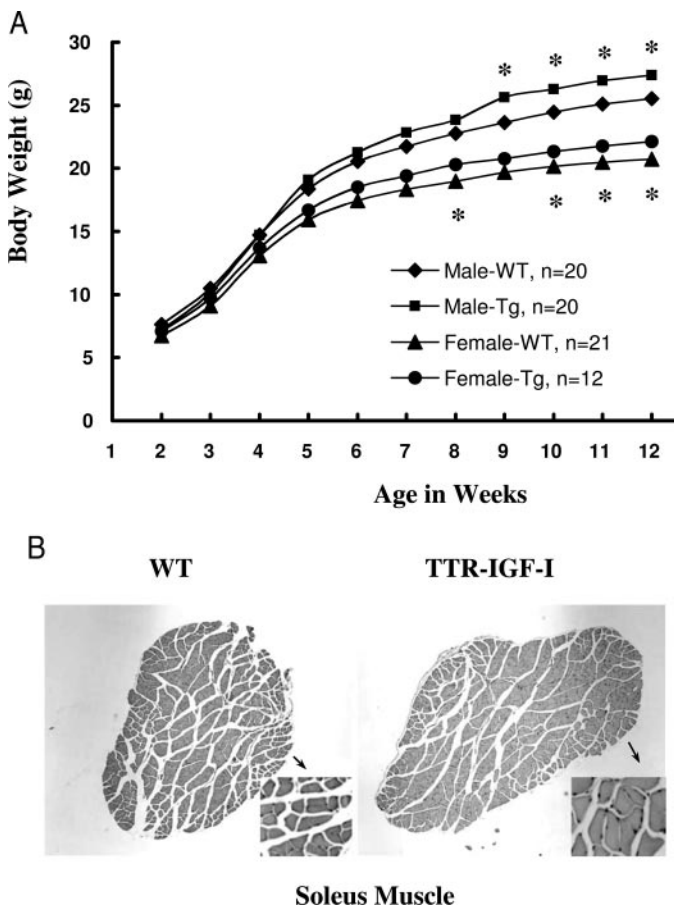


**FIG. 3.** The TTR-IGF-I transgene stimulates body and skeletal muscle growth. **A**, The growth curves of male and female WT and TTR-IGF-I transgenic mice. Average body weight for each genotype group was calculated from the indicated number (*n*) of mice. \*, *P* < 0.05 by *t* test between male or female WT and TTR-IGF-I transgenic (Tg) mice. **B**, The cross-sections of soleus muscles from WT and TTR-IGF-I mice. Note the area of cross-section of WT soleus is smaller than that of TTR-IGF-I soleus. The individual fiber of WT soleus is also much thinner compared with TTR-IGF-I soleus (see *insets*). The quantitative data from multiple mice are presented in Table 2.

soleus and its individual muscle fibers were much thicker in TTR-IGF-I mice compared with WT mice (Fig. 3B, compare the entire cross-sections and the enlarged *insets*). Quantitative analysis of eight WT and six TTR-IGF-I mice further confirmed that the average area and the total number of muscle fibers per soleus section were significantly larger in TTR-IGF-I mice (Table 1). The individual muscle fiber was also much thicker in TTR-IGF-I mice compared with WT mice (Table 1). These results indicate that the increased lean mass in TTR-IGF-I mice is associated with both the increase

**TABLE 1.** TTR-IGF-I transgene stimulates skeletal muscle growth

	No. of mice ( <i>n</i> )	Soleus thickness (pixels)	Fiber counts (per section)	Fiber thickness (pixels/fiber)
WT	6	64,868 ± 5,828	822 ± 53	77.6 ± 8.7
Tg	8	86,059 ± 8,781	912 ± 59	92.4 ± 8.1
<i>P</i> value		<0.0001	<0.05	<0.01

Data are presented as average ± SD. *P* values were calculated by unpaired *t* test, and *P* < 0.05 is considered significantly different.

of muscle fiber numbers and the increase of muscle fiber thickness.

Furthermore, we examined whether expression of the TTR-IGF-I transgene in the liver affects bone growth by measuring femur and tibia lengths in live mice. The average lengths of femur and tibia had no statistical differences between WT and TTR-IGF-I mice when measured at the ages of 5 and 7 wk. However, when measured at the age of 9 wk, both femur and tibia of TTR-IGF-I mice were significantly longer than the femur and tibia lengths of WT mice (Table 2). We also measured the bone density and found that the bone density was identical in WT mice and TTR-IGF-I mice, which was 0.05 ± 0.002 g/cm<sup>2</sup> (*n* = 10 for each group). These results indicate that the elevated level of plasma IGF-I is able to enhance bone growth without additional enhancement of bone density.

#### *TTR-IGF-I mice show a slightly increased glucose tolerance*

It has been shown that reduction of liver-produced IGF-I in mice increases GH, insulin, insulin resistance, and blood glucose levels in mice (24). To examine whether TTR-IGF-I mice have an altered regulation of glucose homeostasis, we compared glucose and insulin levels as well as glucose and insulin tolerance levels in adult male WT and TTR-IGF-I mice. The average blood glucose levels were 153 ± 23 mg/dl (*n* = 13) in WT mice freely accessible to food and 144 ± 16 mg/dl (*n* = 13) in WT mice fasted for 6 h, which were similar to the 159 ± 25 mg/dl (*n* = 19) and 131 ± 21 mg/dl respective values observed in TTR-IGF-I mice under same conditions. The average insulin levels were also comparable in fasted WT and TTR-IGF-I mice, which were 508 ± 327 pg/ml (*n* = 19) and 727 ± 398 pg/ml (*n* = 13) and showed no statistical difference. These results demonstrate that the elevated IGF-I levels in TTR-IGF-I mice do not significantly change glucose and insulin levels in their circulation.

The TTR-IGF-I mice showed a slightly improved glucose tolerance. In the glucose tolerance test, the glucose levels in TTR-IGF-I mice were significantly lower at the 60-min time point compared with WT mice, but no significant differences were observed at other time points (Fig. 4A). In addition, the insulin tolerance test did not reveal any difference between WT and TTR-IGF-I mice (Fig. 4B). These results suggest that the increased IGF-I in TTR-IGF-I mice can slightly enhance glucose tolerance.

**TABLE 2.** Promotion of bone growth by the TTR-IGF-I transgene

	Average bone length (mm) ± SD		
	5 wk	7 wk	9 wk
<b>Femur</b>			
WT	32.40 ± 1.52 (5)	32.34 ± 1.21 (5)	34.68 ± 0.15 (5)
Tg	31.68 ± 0.80 (6)	32.65 ± 2.16 (6)	35.40 ± 0.59 (6)
<i>P</i> value	>0.05	>0.05	<0.05
<b>Tibia</b>			
WT	23.04 ± 1.55 (5)	23.88 ± 1.16 (5)	25.02 ± 0.65 (5)
Tg	22.44 ± 1.11 (6)	24.80 ± 1.89 (6)	26.30 ± 0.54 (6)
<i>P</i> value	>0.05	>0.05	<0.01

Numbers in the parentheses indicate the number of mice measured in that group. Unpaired and two-tailed *t* tests were performed to compare the statistical differences of bone lengths between WT and TTR-IGF-I (Tg) mice. The *P* values for all three age groups are listed. If *P* < 0.05, the difference was considered statistically significant.

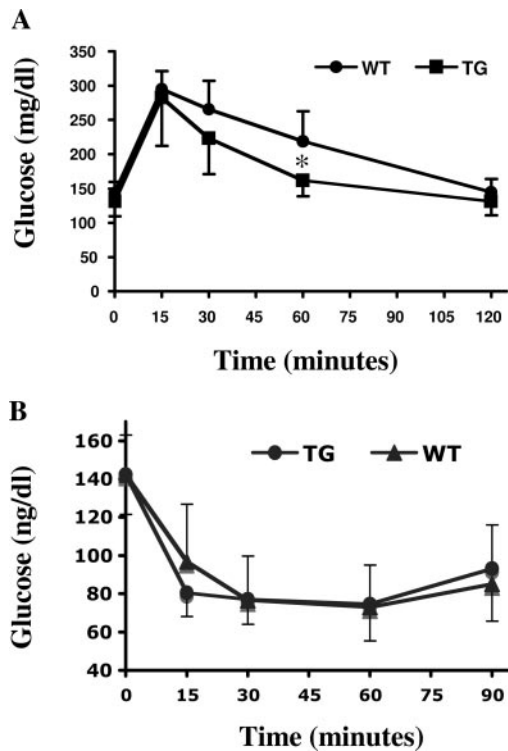


FIG. 4. Glucose and insulin tolerance tests. A, Glucose tolerance test. Glucose was injected into WT and TTR-IGF-I (Tg) mice, and then blood glucose levels were measured at time points indicated. \*,  $P < 0.05$  by one-way ANOVA. B, Insulin tolerance test. Insulin was injected into WT and TTR-IGF-I mice and blood glucose levels were measured at time points indicated. No statistical difference in insulin tolerance was detected between these two groups of mice.

#### TTR-IGF-I transgenic mice are more resistant to the GH-deficient condition

Pegvisomant, a modified GH molecule, is a potent GHR antagonist that disables signal transduction through blocking GHR. Pegvisomant is the most effective pharmacological agent that can normalize IGF-I levels in patients with acromegaly and has also been used to create animal models of acute GH deficiency (25, 26). To define the role of the liver-specific TTR-IGF-I transgene under the condition of GH deficiency, we treated the TTR-IGF-I and WT male mice with PBS (vehicle) or pegvisomant from the age of 3 wk to the age of 8 wk and compared their body weights and body lengths (Fig. 5A). The average body weight and body length of the PBS-treated TTR-IGF-I mice were statistically heavier than WT mice after the age of 5 wk and longer than WT mice as measured at the end of treatment (Fig. 5, B and C), which was consistent with the results observed from the other batch of untreated mice shown in Fig. 3. Pegvisomant treatment significantly inhibited the growth of body weight and body length of both WT and TTR-IGF-I mice compared with the PBS-treated WT and TTR-IGF-I mice. However, the body weight and length of the pegvisomant-treated TTR-IGF-I mice were still statistically heavier and longer than the body weight and length of the pegvisomant-treated WT mice (Fig. 5, B and C). Importantly, the body weight and length of the pegvisomant-treated TTR-IGF-I mice showed no statistical differences from that of the PBS-treated WT mice (Fig. 5, B

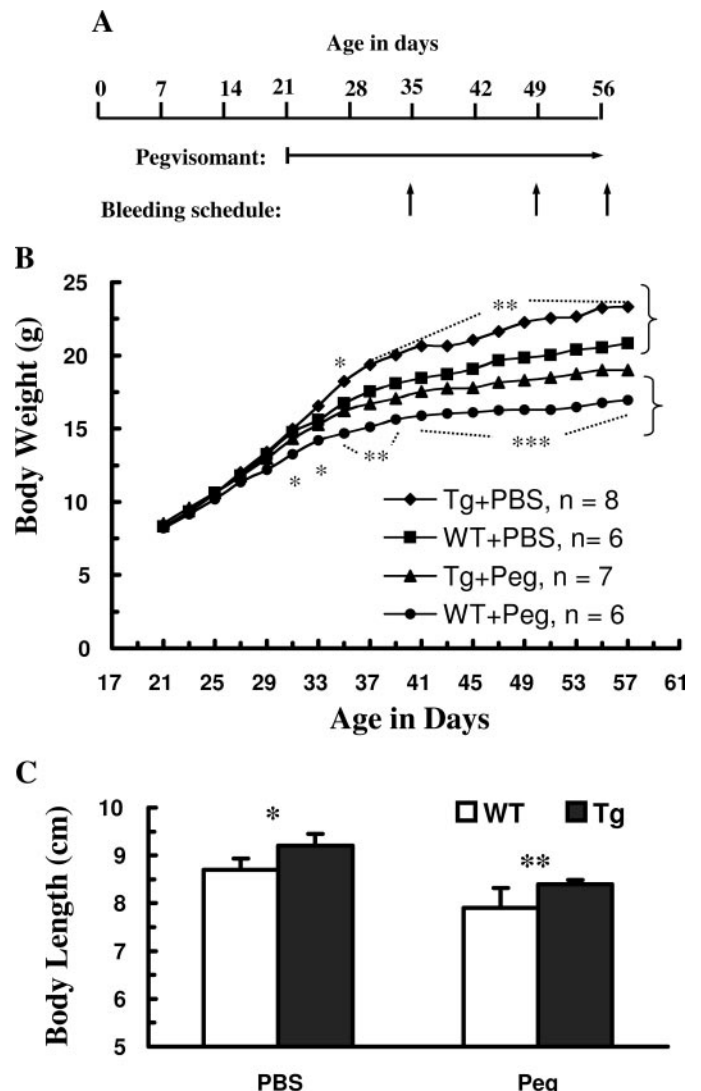


FIG. 5. The pegvisomant-treated TTR-IGF-I mice have heavier body weight and longer body length than pegvisomant-treated WT mice. A, Schedules for pegvisomant treatment and bleeding. Mice were injected with pegvisomant solution every 48 h from the age of 21 d to the age of 56 d. Blood samples were collected at 6, 48, and 24 h after pegvisomant injection at the ages of 35, 49, and 56 d (arrowheads). B, Body weight growth curves of PBS- and pegvisomant (Peg)-treated male WT and TTR-IGF-I transgenic (Tg) mice. The number (n) of mice in each treatment group is indicated. Statistical differences were compared by *t* test: \*,  $P < 0.05$ ; \*\*,  $P < 0.01$ ; \*\*\*,  $P < 0.001$  between PBS-treated WT mice and Tg mice and between Peg-treated WT mice and Tg mice. There are no statistical differences ( $P > 0.05$ ) between PBS-treated WT mice and Peg-treated Tg mice. C, The average body lengths of PBS- and pegvisomant (Peg)-treated WT and TTR-IGF-I (Tg) mice at the age of 56 d. The number of mice in each group is identical to that in B. \*,  $P < 0.05$ ; \*\*,  $P < 0.01$  by *t* test.

and C). These results suggest that mice with the liver-specific and GH-independent expression of the TTR-IGF-I transgene are more resistant to GH deficiency.

To further assess the role of the TTR-IGF-I transgene-generated IGF-I in growth, we measured and compared the organ weights of the IGF-I transgenic mice with WT mice after PBS or pegvisomant treatment. The average brain weight of TTR-IGF-I mice was the same as that of WT mice

regardless of PBS or pegvisomant treatment. However, the average weights of pituitary, heart, liver, kidney, and spleen in the TTR-IGF-I mice were heavier than the weights of respective organs in WT mice after PBS treatment (Table 3). Interestingly, after pegvisomant treatment, the liver and kidney in TTR-IGF-I mice were significantly heavier compared with the liver and kidney in WT mice ( $P < 0.01$  and  $P < 0.001$  by *t* test, respectively). The other organs including pituitary, heart, and spleen in the pegvisomant-treated TTR-IGF-I mice were slightly heavier than that in pegvisomant-treated WT mice, but their differences did not reach statistical significance (Table 3). These results suggest that IGF-I originating from the TTR-IGF-I transgene may preferentially stimulate liver and kidney growth under the condition of GH deficiency.

#### Effects of pegvisomant on GH and IGF-I in TTR-IGF-I mice

It was expected that blockade of GHR by pegvisomant would increase GH levels through the endocrine feedback regulatory mechanism (27). Indeed, GH levels were significantly increased in pegvisomant-treated WT and TTR-IGF-I mice compared with PBS-treated WT and TTR-IGF-I mice (Fig. 6A). Although the difference between GH levels in PBS-treated WT and TTR-IGF-I mice did not reach statistical significance because of limited mice number and single-point analysis in this experiment, the GH levels in PBS-treated TTR-IGF-I mice still showed a lower trend compared with the PBS-treated WT mice. The GH level in pegvisomant-treated TTR-IGF-I mice was lower than that in pegvisomant-treated WT mice, but their difference was also not statistically significant (Fig. 6A). These results indicate that pegvisomant treatment efficiently inhibited the function of GHR in both WT and TTR-IGF-I mice.

To examine the efficiency of pegvisomant-induced GH deficiency on reduction of systemic IGF-I levels and to check whether the pegvisomant-treated TTR-IGF-I mice had higher levels of IGF-I than pegvisomant-treated WT mice, we measured IGF-I concentration in the serum prepared at 6, 24, and 48 h after PBS or pegvisomant injection. As expected, the PBS treatment did not significantly alter the IGF-I levels in WT and TTR-IGF-I mice at all three time points compared with the IGF-I levels of untreated WT and TTR-IGF-I mice (Figs. 6B and 2C). The pegvisomant-treated WT mice exhibited a predictable reduction of the serum IGF-I levels to about 20% of the PBS-treated WT mice. These low levels of IGF-I remained unchanged during the 48-h period from the preceding to the next pegvisomant injection (Fig. 6B), indicating that the pegvisomant successfully resulted in a sustained GH

deficiency in WT mice during the entire 5-wk treatment period. Surprisingly, pegvisomant treatment also significantly reduced the IGF-I levels in TTR-IGF-I mice. However, the IGF-I levels in the pegvisomant-treated TTR-IGF-I mice were 2- to 4-fold higher than the IGF-I levels in pegvisomant-treated WT mice. Furthermore, the average IGF-I level in pegvisomant-treated TTR-IGF-I mice rose significantly at 24 and 48 h after injection compared with their IGF-I levels at 6 h after injection, indicating that the pegvisomant-treated TTR-IGF-I mice can restore their IGF-I levels much faster than the pegvisomant-treated WT mice.

To understand how the pegvisomant treatment affects IGF-I expression, we measured IGF-I mRNA expressed from the endogenous IGF-I gene and the TTR-IGF-I transgene in the liver by RPA. Pegvisomant treatment efficiently and equally reduced the IGF-I mRNA expressed from the endogenous IGF-I gene in WT and TTR-IGF-I mice but did not affect the transgenic IGF-I mRNA expressed from the TTR-IGF-I transgene as normalized to the cyclophilin A control mRNA levels (Fig. 6C). These results suggest that transcriptional inhibition of the endogenous IGF-I gene by the pegvisomant contributes to the significant decrease in IGF-I levels in both WT and TTR-IGF-I mice.

#### Higher expression of IGFBP-3 mRNA and blunted reduction of IGFBP-3 in pegvisomant-treated TTR-IGF-I mice

The majority of IGF-I molecules form ternary complexes with ALS and IGFBP-3 in the circulation (1, 2). These IGF-binding proteins protect IGF-I from degradation and thereby maintain a high systemic IGF-I concentration and its physiological function. To understand why pegvisomant could remarkably reduce the systemic IGF-I levels not only in WT mice but also in the TTR-IGF-I mice without affecting the TTR-IGF-I transgene expression that produced many-fold higher IGF-I mRNA than the endogenous IGF-I gene after pegvisomant treatment, we first examined the ALS mRNA levels in the liver and the ALS protein levels in the serum. RPA analysis using a riboprobe complementary to the mouse ALS mRNA revealed that the pegvisomant treatment severely and equally reduced the ALS expression in both WT and TTR-IGF-I mice compared with PBS treatment (Fig. 7A). Immunoblotting with an ALS-specific antibody detected the ALS protein in the serum of PBS-treated WT and TTR-IGF-I mice but not in the serum of pegvisomant-treated WT and TTR-IGF-I mice (Fig. 7B). Because ALS is a direct target gene of the GH signaling pathway, these results further validated the efficiency of GHR blockade by pegvisomant. These re-

**TABLE 3.** Liver-specific expression of IGF-I selectively increases organ weight

Treatment	n	Average organ weight (mg), mean $\pm$ SD					
		Brain	Pituitary	Heart	Liver	Kidney	Spleen
PBS							
WT	6	432 $\pm$ 18	1.1 $\pm$ 0.17	93 $\pm$ 9	936 $\pm$ 82	262 $\pm$ 34	58 $\pm$ 13
Tg	8	436 $\pm$ 27	1.7 $\pm$ 0.08 <sup>a</sup>	107 $\pm$ 10 <sup>a</sup>	1146 $\pm$ 132 <sup>a</sup>	314 $\pm$ 14 <sup>a</sup>	82 $\pm$ 11 <sup>a</sup>
Pegvisomant							
WT	6	432 $\pm$ 15	1.9 $\pm$ 0.59	94 $\pm$ 6	913 $\pm$ 55	224 $\pm$ 18	83 $\pm$ 33
Tg	7	435 $\pm$ 10	2.4 $\pm$ 0.17	98 $\pm$ 5	1029 $\pm$ 73 <sup>b</sup>	271 $\pm$ 5 <sup>c</sup>	100 $\pm$ 18

<sup>a</sup>  $P < 0.05$ ; <sup>b</sup>  $P < 0.01$ ; <sup>c</sup>  $P < 0.001$  by *t* test comparison between WT and TTR-IGF-I transgenic (Tg) mice treated with PBS or with pegvisomant.

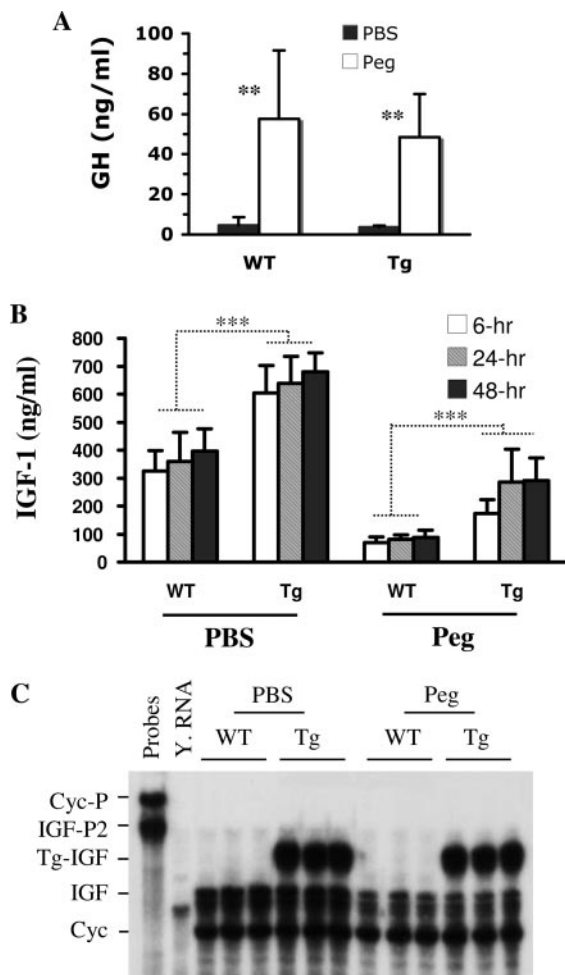


**FIG. 6.** Effects of pegvisomant treatment on GH and IGF-I levels and on endogenous and transgenic IGF-I mRNAs. **A**, Serum GH levels in PBS- and pegvisomant (Peg)-treated WT and TTR-IGF-I transgenic (Tg) mice. Blood samples were collected in 48 h after the preceding Peg injection after mice were treated with Peg for 5 wk. Data are presented as average  $\pm$  SD. The assayed mouse numbers were six and eight for PBS- and Peg-treated WT mice and seven and eight for PBS- and Peg-treated TTR-IGF-I mice. \*\*,  $P < 0.01$  by unpaired  $t$  test between PBS- and Peg-treated groups. The differences between PBS-treated WT and TTR-IGF-I mice and between Peg-treated WT and TTR-IGF-I mice did not reach statistical significance ( $P > 0.05$ ). **B**, Serum IGF-I levels in PBS- and Peg-treated WT and Tg mice 6, 24, and 48 h after Peg injection. The number of mice used for each treatment is identical to the numbers indicated in Fig. 4B. \*\*\*,  $P < 0.001$  by unpaired  $t$  test between WT and Tg groups. **C**, RPA analysis using RNA samples isolated from the liver of PBS- and Peg-treated WT and Tg mice. Note the Peg treatment reduced the endogenous IGF-I mRNA (IGF) but not the transgenic IGF-I mRNA (Tg-IGF). Y.RNA, Yeast RNA (negative control); Cyc-P, cyclophilin probe; IGF-P2, the probe 2 shown in Fig. 1A; Cyc, protected cyclophilin mRNA.

sults also suggest that the significant decrease of IGF-I in pegvisomant-treated WT and TTR-IGF-I mice was associated not only with the reduced expression of the endogenous IGF-I gene but also with the predictable reduction of ALS.

Next, we examined the levels of IGFBP-3 mRNA and protein. The pegvisomant treatment did not change IGFBP-3 mRNA levels in the liver of WT mice compared with vehicle (PBS) treatment (Fig. 7C), indicating that the IGFBP-3 gene is not a direct target gene of the signaling pathway of GH and

its receptor. Surprisingly, the IGFBP-3 mRNA in the liver of pegvisomant-treated TTR-IGF-I mice was increased about 2-fold compared with the pegvisomant-treated WT mice and PBS-treated WT and TTR-IGF-I mice (Fig. 7C). [ $^{125}$ I]IGF-I ligand blotting analysis revealed that serum IGFBP-3 levels were higher in PBS-treated TTR-IGF-I mice than in PBS-treated WT mice (Fig. 7D). Pegvisomant treatment significantly decreased the levels of IGFBP-3 in WT and TTR-IGF-I mice, presumably because of the reduction of ALS (7). However, the levels of IGFBP-3 were much higher in pegvisomant-treated TTR-IGF-I mice than in pegvisomant-treated WT mice (Fig. 7D). These results demonstrate that expression of the liver-specific TTR-IGF-I transgene is able to up-regulate IGFBP-3 mRNA under GHR-dysfunction conditions and counterbalance the decrease of IGFBP-3 caused by GH deficiency, which in turn helps to maintain IGF-I levels in the circulation.

## Discussion

In this study, the TTR-IGF-I transgenic mouse line was generated to study the role of liver-produced IGF-I in the regulation of the GH/IGF-I axis and somatic growth. In this mouse line, the TTR-IGF-I transgene was not regulated by GH, and it was exclusively overexpressed in the liver. Circulating IGF-I levels in these transgenic mice were increased 50–60% under normal physiological conditions. More importantly, the IGF-I produced in the liver from the TTR-IGF-I transgene was secreted into the circulation and was biologically active because it suppressed GH levels and promoted increases in body weight, organ weight, lean mass, body length, and bone length. The lean mass increase resulted from both the enlarged muscle fiber and the increased number of muscle fibers. Therefore, our analysis clearly demonstrate that elevated serum IGF-I originating from a liver-specific TTR-IGF-I transgene can moderately stimulate overall postnatal somatic growth.

We also showed that the TTR-IGF-I transgenic mice have a slightly improved glucose tolerance without significant changes of their glucose and insulin levels under normal feeding and fast conditions. Because GH plays a role in regulation of insulin resistance (24), the improved glucose tolerance in TTR-IGF-I mice may be a result of down-regulated GH levels in these mice. However, it is also possible that the elevated IGF-I stimulates glucose uptake by peripheral tissues.

To our knowledge, the TTR-IGF-I transgenic mouse line is the first line that exclusively overexpresses transgenic IGF-I in the liver. Because the liver is the major organ responsible for production of the circulating IGF-I, this transgenic mouse model should be particularly useful for studying the endocrine function of IGF-I. One of the previously established IGF-I transgenic mouse lines used the promoter of avian skeletal  $\alpha$ -actin to direct the expression of human IGF-I in the striated muscle. The epitopic expression of the IGF-I transgene in these transgenic mice resulted in myofiber hypertrophy with no effect on the circulating IGF-I levels and body weight (28). Another documented IGF-I transgenic mouse line was developed by using the mouse metallothionein I promoter. This mouse line overexpressed human IGF-I in

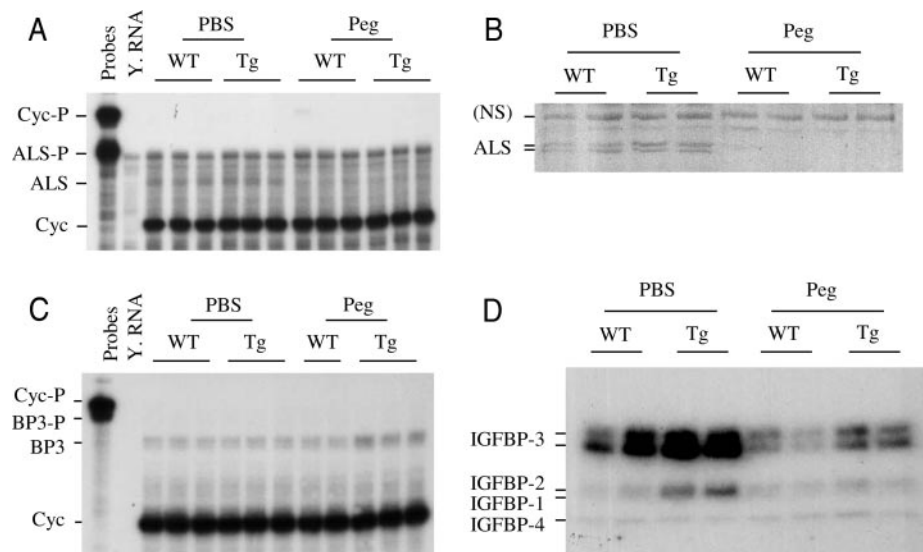


FIG. 7. Analysis of ALS and IGFBP-3 mRNA and protein. A, RPA of ALS mRNA in the liver. The cyclophilin A probe (Cyc-P), the ALS probe (ALS-P), and the protected ALS and cyclophilin A (Cyc) mRNA bands are indicated. A long-time exposure of the x-ray film to the RPA gel was required to see the protected weak ALS mRNA band because of its low expression level, which made an undigested ALS-P band and certain weak nonspecific background bands visible. Note the significant reduction of the ALS band intensity observed in the pegvisomant (Peg)-treated WT and TTR-IGF-I transgenic (Tg) mice. B, Immunoblotting analysis of the serum ALS protein in PBS- and Peg-treated WT and Tg mice. Note the absence of the ALS band in the Peg-treated mice. A nonspecific band (NS) is shown to serve as a reference for relative loading of total protein. C, RPA of IGFBP-3 mRNA in the liver. The IGFBP-3 probe (BP3-P) and the protected IGFBP-3 mRNA (BP3) are indicated. Note the increased intensity of the BP3 mRNA band in Peg-treated Tg mice. The protected cyclophilin A (Cyc) serves as an endogenous control of RNA amount. D, [ $^{125}$ I]IGF-I ligand blotting analysis of IGF-binding proteins in PBS- and Peg-treated WT and Tg mice. Note that IGFBP-3 is higher in Peg-treated transgenic mice than in Peg-treated WT mice. IGFBP-4 is identical in all mice.

most tissues and manifested a 1.5-fold increase in circulating IGF-I levels and a 1.3-fold increase in body weight (29). Although the results from this transgenic mouse line demonstrated that elevated IGF-I played an important role in the control of somatic growth, it was not able to distinguish the contribution of the elevated plasma IGF-I from the contribution of locally produced IGF-I to the transgene-enhanced somatic growth.

Interestingly, although the TTR-IGF-I transgene was expressed several-fold higher than the endogenous IGF-I gene in the liver, the plasma IGF-I levels were increased only 50–60% in untreated or 65–100% in PBS-treated TTR-IGF-I mice compared with WT mice (Figs. 2C and 6B). This could be attributed to the limiting concentrations of ALS and IGFBP-3 in the circulation because they are key factors that determine IGF-I stability. We noticed that the IGFBP-3 levels were slightly higher in PBS-treated TTR-IGF-I mice compared with PBS-treated WT mice (Fig. 7D), suggesting that the increased production of IGF-I also extended the IGFBP-3 half-life in the circulation because IGFBP-3 mRNA levels were unaltered under this condition. Therefore, the plasma ALS concentration may be the major limiting factor for final levels of IGF-I increase in TTR-IGF-I mice. This notion is further supported by the significant reduction of plasma IGF-I levels in TTR-IGF-I mice after pegvisomant treatment, where ALS was severely reduced, whereas the expression of the TTR-IGF-I transgene was unaffected in these mice with GHR dysfunction.

In this study, we have used pegvisomant to determine whether transgenic non-GH-regulated IGF-I can alter phenotypes associated with loss of GH action. Under the con-

dition of GHR dysfunction caused by pegvisomant treatment, we found that ALS was diminished from the circulation of both WT and TTR-IGF-I mice. This was an expected effect because ALS is a direct target of the GHR signaling pathway, and blockade of GHR severely reduced ALS mRNA expression in the liver (1, 2, 7). As expected, GHR dysfunction also caused a significant reduction of IGF-I mRNA transcribed from the endogenous IGF-I gene in the liver of both WT and TTR-IGF-I mice but did not alter the IGF-I mRNA transcribed from the TTR-IGF-I transgene in the transgenic mice. In this case, transgene expression resulted in 2- to 3-fold higher IGF-I concentrations in TTR-IGF-I mice compared with WT mice after pegvisomant treatment. Consequently, the serum IGF-I levels were reduced much less in TTR-IGF-I mice than in WT mice after pegvisomant treatment, although IGF-I was significantly reduced in pegvisomant-treated WT and TTR-IGF-I mice compared with PBS-treated WT and TTR-IGF-I mice, respectively.

In the pegvisomant-treated WT mice, the expression of IGFBP-3 mRNA in the liver was unaffected, indicating that IGFBP-3 is not a direct target of the GH/GHR signaling pathway *in vivo*. However, the plasma IGFBP-3 levels were drastically reduced in pegvisomant-treated WT mice, likely because of its impaired stability after the severe reduction of ALS and IGF-I as observed in mice lacking ALS or lacking liver-produced IGF-I (6, 7, 14). In the pegvisomant-treated TTR-IGF-I mice, the plasma IGFBP-3 levels were reduced compared with the PBS-treated TTR-IGF-I mice. However, the plasma IGFBP-3 levels in the pegvisomant-treated TTR-IGF-I mice were about 2-fold higher than in the pegvisomant-treated WT mice. These results were consistent with those of

a previous study showing that the IGFBP-3 levels were higher in the GH-deficient mice harboring a widely expressed IGF-I transgene compared with GH-deficient mice (30). The higher IGFBP-3 levels in pegvisomant-treated TTR-IGF-I mice can be attributed to two contributions. First, the consistently available IGF-I produced from the transgene should stabilize IGFBP-3 in the circulation and extend its half-life; second, the IGFBP-3 mRNA expression was increased in pegvisomant-treated TTR-IGF-I mice compared with pegvisomant-treated WT mice as well as PBS-treated TTR-IGF-I and WT mice. Interestingly, the transgene-produced IGF-I stimulates IGFBP-3 mRNA expression in the liver only under the condition of GHR dysfunction. Consequently, the pegvisomant-treated TTR-IGF-I mice with better-maintained plasma IGF-I and IGFBP-3 levels manifested a higher resistance to GHR dysfunction or GH deficiency, including a heavier body weight, longer body length, and a maintained IGF-I/IGF-IR signaling pathway in target tissues.

At the present time, it is not clear why the increase of IGFBP-3 transcription in the liver appeared only in the pegvisomant-treated TTR-IGF-I mice and how the TTR-IGF-I transgene-produced IGF-I stimulated the increase in IGFBP-3 mRNA under the condition of GHR dysfunction. Because pegvisomant treatment had no effect on the TTR-IGF-I transgene expression but significantly reduced serum ALS and IGFBP-3 concentrations, it is possible that the unaltered synthesis and secretion of transgenic IGF-I in the liver created an excess ratio of IGF-I to its binding proteins, ALS and IGFBP-3, which at least locally increased the free IGF-I concentration. The locally increased free IGF-I might stimulate IGFBP-3 expression in hepatic nonparenchymal cells and endothelial cells because parenchymal liver cells do not express IGF-IR and IGFBP-3 (1, 8).

Clinical studies have found a positive correlation between circulating IGF-I concentrations and the risk of breast cancer among premenopausal but not postmenopausal women (31), suggesting that plasma IGF-I levels may play an important role in ovarian steroids-promoted breast tumorigenesis. Other studies also have suggested a positive correlation between the circulating IGF-I levels and the relative risks of colon, prostate, and lung cancers (32–35). These clinical observations have been mimicked in mouse models, where lowering IGF-I inhibits growth of an array of different cancers (36). We believe that the TTR-IGF-I transgenic mice will be very useful for studying the role and molecular mechanisms of the circulating IGF-I in promotion of carcinogenesis. Furthermore, the TTR-IGF-I mice also will be valuable to be used in conjunction with other genetically manipulated mouse models to investigate the endocrine function of the liver-generated IGF-I in regulation of many physiological processes. For instance, the TTR-IGF-I mice can be crossed with the IGF-I knockout mice to produce IGF-I knockout mice harboring the liver-specific IGF-I transgene. This bigenic animal model would help to address the question as to how the circulating IGF-I regulates somatic growth and targets different tissues that do not express endogenous IGF-I through an endocrine mechanism.

## Acknowledgments

We thank Dr. Francesco J. DeMayo and the Baylor Transgenic Core for microinjection and Pfizer for providing pegvisomant.

Received December 5, 2005. Accepted May 8, 2006.

Address all correspondence and requests for reprints to: Jianming Xu, Ph.D., Department of Molecular and Cellular Biology, Baylor College of Medicine, One Baylor Plaza, Houston, Texas 77030. E-mail: jxu@bcm.tmc.edu.

This work was supported in part by grants from the National Institutes of Health: DK58242 and CA119689 to J.X., CA94118 and P01CA30195 to A.L. J.X. is a recipient of an American Cancer Society Scholar Award. A.L. is a recipient of a Chao Scholar Award. R.D. was supported in part by a Training Program in Molecular Endocrinology (DK07696).

Author disclosure summary: L.L., R.D., S.Z., O.B., and J.X. have nothing to declare. A.L. received lecture fees and consulting fees from Pfizer and Bristol Myers Squibb.

## References

1. Stewart CE, Rotwein P 1996 Growth, differentiation, and survival: multiple physiological functions for insulin-like growth factors. *Physiol Rev* 76:1005–1026
2. Jones JI, Clemmons DR 1995 Insulin-like growth factors and their binding proteins: biological actions. *Endocr Rev* 16:3–34
3. Liu JP, Baker J, Perkins AS, Robertson EJ, Efstratiadis A 1993 Mice carrying null mutations of the genes encoding insulin-like growth factor I (Igf-1) and type 1 IGF receptor (Igf1r). *Cell* 75:59–72
4. Powell-Braxton L, Hollingshead P, Warburton C, Dowd M, Pitts-Meek S, Dalton D, Gillett N, Stewart TA 1993 IGF-I is required for normal embryonic growth in mice. *Genes Dev* 7:2609–2617
5. Modric T, Silha JV, Shi Z, Gui Y, Suwanichkul A, Durham SK, Powell DR, Murphy LJ 2001 Phenotypic manifestations of insulin-like growth factor-binding protein-3 overexpression in transgenic mice. *Endocrinology* 142:1958–1967
6. Yakar S, Liu JL, Stannard B, Butler A, Accili D, Sauer B, LeRoith D 1999 Normal growth and development in the absence of hepatic insulin-like growth factor I. *Proc Natl Acad Sci USA* 96:7324–7329
7. Ueki I, Ooi GT, Tremblay ML, Hurst KR, Bach LA, Boisclair YR 2000 Inactivation of the acid labile subunit gene in mice results in mild retardation of postnatal growth despite profound disruptions in the circulating insulin-like growth factor system. *Proc Natl Acad Sci USA* 97:6868–6873
8. Chin E, Zhou J, Dai J, Baxter RC, Bondy CA 1994 Cellular localization and regulation of gene expression for components of the insulin-like growth factor ternary binding protein complex. *Endocrinology* 134:2498–2504
9. Silha JV, Murphy LJ 2002 Insights from insulin-like growth factor binding protein transgenic mice. *Endocrinology* 143:3711–3714
10. Schoenle E, Zapf J, Humbel RE, Froesch ER 1982 Insulin-like growth factor I stimulates growth in hypophysectomized rats. *Nature* 296:252–253
11. Guler HP, Zapf J, Scheiwiller E, Froesch ER 1988 Recombinant human insulin-like growth factor I stimulates growth and has distinct effects on organ size in hypophysectomized rats. *Proc Natl Acad Sci USA* 85:4889–4893
12. Skottner A, Clark RG, Fryklund L, Robinson IC 1989 Growth responses in a mutant dwarf rat to human growth hormone and recombinant human insulin-like growth factor I. *Endocrinology* 124:2519–2526
13. Butler AA, LeRoith D 2001 Tissue-specific versus generalized gene targeting of the *igf1* and *igf1r* genes and their roles in insulin-like growth factor physiology. *Endocrinology* 142:1685–1688
14. Yakar S, Rosen CJ, Beamer WG, Ackert-Bicknell CL, Wu Y, Liu JL, Ooi GT, Setser J, Frystyk J, Boisclair YR, LeRoith D 2002 Circulating levels of IGF-1 directly regulate bone growth and density. *J Clin Invest* 110:771–781
15. Wang Y, DeMayo FJ, Tsai SY, O'Malley BW 1997 Ligand-inducible and liver-specific target gene expression in transgenic mice. *Nat Biotechnol* 15:239–243
16. Xu J, Liao L, Ning G, Yoshida-Komiya H, Deng C, O'Malley BW 2000 The steroid receptor coactivator SRC-3 (p/CIP/RAC3/AIB1/ACTR/TRAM-1) is required for normal growth, puberty, female reproductive function, and mammary gland development. *Proc Natl Acad Sci USA* 97:6379–6384
17. Brommage R 2003 Validation and calibration of DEXA body composition in mice. *Am J Physiol Endocrinol Metab* 285:E454–E459
18. Fernandez AM, Dupont J, Farrar RP, Lee S, Stannard B, LeRoith D 2002 Muscle-specific inactivation of the IGF-I receptor induces compensatory hyperplasia in skeletal muscle. *J Clin Invest* 109:347–355
19. McCusker RH, Clemmons DR 1988 Insulin-like growth factor binding protein secretion by muscle cells: effect of cellular differentiation and proliferation. *J Cell Physiol* 137:505–512
20. Lee AV, Zhang P, Ivanova M, Bonnette S, Oesterreich S, Rosen JM, Grimm

- S, Hovey RC, Vonderhaar BK, Kahn CR, Torres D, George J, Mohsin S, Allred DC, Hadsell DL 2003 Developmental and hormonal signals dramatically alter the localization and abundance of insulin receptor substrate proteins in the mammary gland. *Endocrinology* 144:2683–2694
21. Yan C, Costa RH, Darnell Jr JE, Chen JD, Van Dyke TA 1990 Distinct positive and negative elements control the limited hepatocyte and choroid plexus expression of transthyretin in transgenic mice. *EMBO J* 9:869–878
  22. Wu H, Wade M, Krall L, Grisham J, Xiong Y, Van Dyke T 1996 Targeted in vivo expression of the cyclin-dependent kinase inhibitor p21 halts hepatocyte cell-cycle progression, postnatal liver development and regeneration. *Genes Dev* 10:245–260
  23. Chung JH, Whiteley M, Felsenfeld G 1993 A 5' element of the chicken  $\beta$ -globin domain serves as an insulator in human erythroid cells and protects against position effect in *Drosophila*. *Cell* 74:505–514
  24. Yakar S, Setser J, Zhao H, Stannard B, Haluzik M, Glatt V, Bouxsein ML, Kopchick JJ, LeRoith D 2004 Inhibition of growth hormone action improves insulin sensitivity in liver IGF-1-deficient mice. *J Clin Invest* 113:96–105
  25. Trainer PJ, Drake WM, Katznelson L, Freda PU, Herman-Bonert V, van der Lely AJ, Dimaraki EV, Stewart PM, Friend KE, Vance ML, Besser GM, Scarlett JA, Thorner MO, Parkinson C, Klibanski A, Powell JS, Barkan AL, Sheppard MC, Malsonado M, Rose DR, Clemmons DR, Johannsson G, Bengtsson BA, Stavrou S, Kleinberg DL, Cook DM, Phillips LS, Bidlingmaier M, Strasburger CJ, Hackett S, Zib K, Bennett WF, Davis RJ 2000 Treatment of acromegaly with the growth hormone-receptor antagonist pegvisomant. *N Engl J Med* 342:1171–1177
  26. van Neck JW, Dits NF, Cingel V, Hoppenbrouwers IA, Drop SL, Flyvbjerg A 2000 Dose-response effects of a new growth hormone receptor antagonist (B2036-PEG) on circulating, hepatic and renal expression of the growth hormone/insulin-like growth factor system in adult mice. *J Endocrinol* 167:295–303
  27. Zhou Y, Xu BC, Maheshwari HG, He L, Reed M, Lozykowski M, Okada S, Cataldo L, Coschigamo K, Wagner TE, Baumann G, Kopchick JJ 1997 A mammalian model for Laron syndrome produced by targeted disruption of the mouse growth hormone receptor/binding protein gene (the Laron mouse). *Proc Natl Acad Sci USA* 94:13215–13220
  28. Coleman ME, DeMayo F, Yin KC, Lee HM, Geske R, Montgomery C, Schwartz RJ 1995 Myogenic vector expression of insulin-like growth factor I stimulates muscle cell differentiation and myofiber hypertrophy in transgenic mice. *J Biol Chem* 270:12109–12116
  29. Mathews LS, Hammer RE, Behringer RR, D'Ercole AJ, Bell GI, Brinster RL, Palmiter RD 1988 Growth enhancement of transgenic mice expressing human insulin-like growth factor I. *Endocrinology* 123:2827–2833
  30. Camacho-Hubner C, Clemmons DR, D'Ercole AJ 1991 Regulation of insulin-like growth factor (IGF) binding proteins in transgenic mice with altered expression of growth hormone and IGF-I. *Endocrinology* 129:1201–1206
  31. Hankinson SE, Willett WC, Colditz GA, Hunter DJ, Michaud DS, Deroo B, Rosner B, Speizer FE, Pollak M 1998 Circulating concentrations of insulin-like growth factor-I and risk of breast cancer. *Lancet* 351:1393–1396
  32. Ma J, Pollak MN, Giovannucci E, Chan JM, Tao Y, Hennekens CH, Stampfer MJ 1999 Prospective study of colorectal cancer risk in men and plasma levels of insulin-like growth factor (IGF)-I and IGF-binding protein-3. *J Natl Cancer Inst* 91:620–625
  33. Chan JM, Stampfer MJ, Giovannucci E, Gann PH, Ma J, Wilkinson P, Hennekens CH, Pollak M 1998 Plasma insulin-like growth factor-I and prostate cancer risk: a prospective study. *Science* 279:563–566
  34. Wolk A, Mantzoros CS, Andersson SO, Bergstrom R, Signorello LB, Lagiou P, Adami HO, Trichopoulos D 1998 Insulin-like growth factor 1 and prostate cancer risk: a population-based, case-control study. *J Natl Cancer Inst* 90:911–915
  35. Yu H, Spitz MR, Mistry J, Gu J, Hong WK, Wu X 1999 Plasma levels of insulin-like growth factor-I and lung cancer risk: a case-control analysis. *J Natl Cancer Inst* 91:151–156
  36. Yakar S, Leroith D, Brodt P 2005 The role of the growth hormone/insulin-like growth factor axis in tumor growth and progression: lessons from animal models. *Cytokine Growth Factor Rev* 16:407–420

*Endocrinology* is published monthly by The Endocrine Society (<http://www.endo-society.org>), the foremost professional society serving the endocrine community.